IS26-mediated amplification of bla_{OXA-1} and $bla_{CTX-M-15}$ with concurrent outer membrane porin disruption associated with *de novo* carbapenem resistance in a recurrent bacteraemia cohort

William C. Shropshire[1,2], Samuel L. Aitken [2,3], Reed Pifer[4], Jiwoong Kim[5], Micah M. Bhatti[6], Xiqi Li[7], Awdhesh Kalia[8], Jessica Galloway-Peña[2,7,9], Pranoti Sahasrabhojane[7], Cesar A. Arias[1,2,10,11], David E. Greenberg[2,12,13], Blake M. Hanson[1,2] and Samuel A. Shelburne [2,7,9]*

[1]Center for Infectious Diseases, School of Public Health, University of Texas Health Science Center, Houston, TX 77030, USA; [2]Center for Antimicrobial Resistance and Microbial Genomics, Division of Infectious Diseases, University of Texas Health Science Center at Houston McGovern Medical School, Houston, TX 77030, USA; [3]Division of Pharmacy, MD Anderson Cancer Center, Houston, TX 77030, USA; [4]Division of Infectious Diseases, Department of Internal Medicine, University of Texas Health Science Center at Houston, McGovern Medical School at Houston, Houston, TX 77030, USA; [5]Department of Bioinformatics, UT Southwestern Medical Center, Dallas, TX 75390, USA; [6]Department of Laboratory Medicine, MD Anderson Cancer Center, Houston, TX 77030, USA; [7]Department of Infectious Diseases, MD Anderson Cancer Center, Houston, TX 77030, USA; [8]Graduate Program in Diagnostic Genetics, School of Health Professions, The University of Texas MD Anderson Cancer Center, Houston, TX, USA; [9]Department of Genomic Medicine, MD Anderson Cancer Center, Houston, TX 77030, USA; [10]Department of Microbiology and Molecular Genetics, University of Texas McGovern Medical School at Houston, Houston, TX 77030, USA; [11]Molecular Genetics and Antimicrobial Resistance Unit, International Center for Microbial Genomics, Universidad El Bosque, Bogotá, Ak. 9#131a2, Colombia; [12]Department of Internal Medicine, UT Southwestern, Dallas, TX 75390, USA; [13]Department of Microbiology, UT Southwestern, Dallas, TX 75390, USA

*Corresponding author. E-mail: sshelburne@mdanderson.org

Background: Approximately half of clinical carbapenem-resistant Enterobacterales (CRE) isolates lack carbapenem-hydrolysing enzymes and develop carbapenem resistance through alternative mechanisms.

Objectives: To elucidate development of carbapenem resistance mechanisms from clonal, recurrent ESBL-positive Enterobacterales (ESBL-E) bacteraemia isolates in a vulnerable patient population.

Methods: This study investigated a cohort of ESBL-E bacteraemia cases in Houston, TX, USA. Oxford Nanopore Technologies long-read and Illumina short-read sequencing data were used for comparative genomic analysis. Serial passaging experiments were performed on a set of clinical ST131 *Escherichia coli* isolates to recapitulate *in vivo* observations. Quantitative PCR (qPCR) and qRT–PCR were used to determine copy number and transcript levels of β-lactamase genes, respectively.

Results: Non-carbapenemase-producing CRE (non-CP-CRE) clinical isolates emerged from an ESBL-E background through a concurrence of primarily IS26-mediated amplifications of bla_{OXA-1} and $bla_{CTX-M-1}$ group genes coupled with porin inactivation. The discrete, modular translocatable units (TUs) that carried and amplified β-lactamase genes mobilized intracellularly from a chromosomal, IS26-bound transposon and inserted within porin genes, thereby increasing β-lactamase gene copy number and inactivating porins concurrently. The carbapenem resistance phenotype and TU-mediated β-lactamase gene amplification were recapitulated by passaging a clinical ESBL-E isolate in the presence of ertapenem. Clinical non-CP-CRE isolates had stable carbapenem resistance phenotypes in the absence of ertapenem exposure.

Conclusions: These data demonstrate IS26-mediated mechanisms underlying β-lactamase gene amplification with concurrent outer membrane porin disruption driving emergence of clinical non-CP-CRE. Furthermore, these amplifications were stable in the absence of antimicrobial pressure. Long-read sequencing can be utilized to identify unique mobile genetic element mechanisms that drive antimicrobial resistance.

Introduction

Carbapenem-resistant Enterobacterales (CRE) infections are an emerging global health priority and among the most serious antimicrobial resistance (AMR) threats.[1] Carbapenem resistance can develop due to acquisition of enzymes that hydrolyse carbapenems, known as carbapenemases, as well as through outer membrane permeability changes and/or drug efflux activity that decrease intracellular carbapenem concentrations.[2] Globally, carbapenem-producing Enterobacterales (CPE) remain the most predominant CRE subset group.[2] Nevertheless, while most CRE research has focused on characterizing CPE,[2,3] recent clinical and molecular epidemiology studies indicate up to 50% of CRE isolates can be non-carbapenemase producers, suggesting that a substantial proportion of CRE isolates develop carbapenem resistance through alternative mechanisms.[4,5] Although the contribution of non-carbapenemase-producing CRE (non-CP-CRE) to the overall CRE population can be highly variable by geographical location as well as patient population, many countries report non-CP-CRE as a highly prevalent CRE subset group, suggesting a global impact of these understudied pathogens.[6–8]

Non-CP-CRE mechanistic studies have been conducted in both basic and clinical research settings.[9–14] Clinical non-CP-CRE isolates generally carry ESBL or AmpC-like enzymes with concomitant mutations that alter porin function.[9,10] Similarly, laboratory passaging of ESBL-positive Enterobacterales (ESBL-E) strains has indicated that development of carbapenem resistance requires both an ESBL and a decrease in outer membrane porin function.[11–14] Additionally, augmented production of β-lactamases without known carbapenemase activity has important effects on carbapenem susceptibility in porin-deficient backgrounds.[13,14] Thus, it is generally thought that non-CP-CRE strains arise from precursor strains producing either an ESBL or AmpC enzyme. However, it is likely that transition from ESBL-E to non-CP-CRE primarily occurs during colonization such that having paired ESBL-E and non-CP-CRE clinical isolates is rare.[9–17] Thus, there remains a knowledge gap regarding mechanisms by which non-CP-CRE mechanisms evolve in patient populations.

Herein, we sought to address how ESBL-E isolates transition to CRE in the clinical setting by systematically studying a cohort of ESBL-E bacteraemia isolates to assess CRE prevalence and characterize mechanisms of CRE emergence. Through the application of long-read and short-read WGS technologies on serial clinical isolates, as well as through serial passaging experiments, we sought to generate insights into how outer membrane porins become inactivated, as well as characterize β-lactamase amplification mechanisms within a patient cohort.

Materials and methods

Study design and clinical data abstraction

A retrospective review of patients with ESBL-E bacteraemia hospitalized from January 2015 to July 2016 was conducted at MD Anderson Cancer Center (MDACC) in Houston, TX, USA. All patients with one or more episodes of ESBL-E bacteraemia who were 18 years of age or older were eligible for inclusion. Clinical and demographic characteristics were extracted from electronic medical records and recorded using REDCap software (Vanderbilt University, Nashville, TN, USA).[18] A waiver of informed consent to collect clinical data from electronic medical records and analyse the isolates was provided by the MDACC IRB (PA15-0799).

Isolate characterization and antimicrobial susceptibility testing

Blood culture isolates are routinely saved at MDACC and stored at −80°C. Carbapenem resistance was defined using CLSI criteria as resistance to either ertapenem or meropenem.[19] Recurrent Enterobacterales bacteraemia was defined as identification of the same species in blood culture at any point during the follow-up period following at least one negative blood culture and completion of an antibiotic treatment regimen.

Antibiotic susceptibility testing was performed per routine clinical laboratory practice using an automated system (VITEK 2, bioMérieux, Marcy L'Étoile, France) with additional testing performed as needed using individual antibiotic gradient strips (Etest, bioMérieux). ESBL production was assessed per routine laboratory practice on *Escherichia coli, Klebsiella pneumoniae* and *Klebsiella oxytoca* isolates that were resistant to one or more oxyimino-cephalosporins (e.g. cefotaxime, ceftriaxone or ceftazidime) using either the ESBL Etest (bioMérieux) or the Rapid ESBL Screen kit (ROSCO, Taastrup, Denmark). Carbapenemase production was evaluated in the clinical laboratory for any Enterobacterales isolate resistant to one or more of the carbapenems using the Neo-Rapid CARB kit (ROSCO) according to the manufacturer's instructions.

WGS and normalized coverage depth analysis

All available isolates from recurrent bacteraemia patients underwent WGS via Illumina HiSeq as described previously.[20] Normalized coverage depth of short-read mapping to individual genes or genome regions of interest was quantitated relative to the average short-read mapping depth for the PubMLST *E. coli* housekeeping gene schema using a suite of bioinformatic tools (bwa v0.7.17, minimap2 v2.2.17, SAMtools v1.9, bedtools v2.27.1) to infer approximate copy numbers.[21–23] Serial isolates that developed a non-CP-CRE phenotype, isolates used in serial passaging experiments and non-CP-CRE isolates from a previous study[20] underwent Oxford Nanopore Technologies (ONT) long-read sequencing. A custom Python script was used to generate hybrid, consensus assemblies using the Flye assembler v2.5[24] (https://github.com/wshropshire/flye_hybrid_assembly_pipeline). A description of the hybrid assembly pipeline is available in the Supplementary methods, available as Supplementary data at *JAC* Online. ONT assembly metrics are provided in Table S1.

Clonality analysis

Phylogenetic analysis, *in silico* MLST and variant calling of serial isolates compared with the index strain genome were used to determine clonality. Roary v3.12.0[25] was used to perform a core-gene alignment with the aligner tool PRANK.[25,26] A maximum-likelihood (ML) phylogenetic tree using RAxML v8.2.12[27] was built using the core-gene alignment. *In silico* MLST was performed using mlst v2.15.1 (https://github.com/tseemann/mlst).[28] Recurrent isolates that became non-CP-CRE were checked for clonality using the variant-calling pipeline tool Snippy v4.3.6 (https://github.com/tseemann/snippy) using the consensus assemblies of the index isolates as references.

Genome annotation, AMR gene and mobile genetic element (MGE) identification

Genome annotation was performed using Prokka v1.14.0.[29] ABRicate (https://github.com/tseemann/abricate), using the Comprehensive Antibiotic Resistance Database (CARD),[30] and PlasmidFinder[31] were used to search for AMR determinants, such as carbapenemases, and plasmid signatures, respectively. Annotated Prokka gbk files were used to characterize ORFs of interest. CARD, PlasmidFinder, ISFinder[32] and BLAST webtools were utilized during manual inspection of the assemblies. SVAnts v0.1[33] (https://

github.com/EpiBlake/SVAnts) was used to investigate subsets of ONT long reads.

β-lactamase gene copy number, transcript level and impact of β-lactamase expression on susceptibility analysis

Quantitative PCR (qPCR) and qRT–PCR were used to assess DNA copy number and RNA transcript levels, respectively. qPCR and qRT–PCR primers and probe sequences are provided in Table S2. The DNA levels of bla_{OXA-1} and $bla_{CTX-M-1}$ group genes were determined relative to the *rpsL* control gene using the ΔCt method as described previously.[14] A full description of the methods used for copy number and gene transcript level quantification can be found in the Supplementary methods. For the purposes of β-lactamase cloning and expression analysis, the ORFs of β-lactamases were amplified from genomic DNA using Q5 polymerase with the primers listed in Table S2. Additional experiment parameters and conditions are provided in the Supplementary methods.

Serial passaging experiments on clinical E. coli ST131 bacteraemia isolates

Two individual passaging experiments of the Patient 4 index strain, i.e. isolate 4A, with antibiotic selection were performed in LB broth under shaking conditions at 37°C. For the first passaging experiment, cells were collected on four consecutive days (strains 4A_1 to 4A_4) while continuing to passage at an ertapenem concentration of 32 mg/L. For the second set of passaging experiments, cells were collected on the first day that the ertapenem MIC reached ≥32 mg/L, serially diluted onto agar plates and two different isolates were studied to assess for heterogeneity (strains 4A_H1 and 4A_H2). Additional serial passaging experiments were conducted using ertapenem-resistant patient strains 4C and 4D in the absence of antibiotic selection, to determine the stability of the amplified translocatable units, with a protocol adapted from previously published methods.[34] Additional experimental conditions are included in the Supplementary methods.

Statistical analyses

All statistical analyses were performed using Stata v13.1 (StataCorp LP, College Station, TX, USA). Bivariate comparisons between patients with a single bacteraemia episode and those with recurrent bacteraemia were made with Wilcoxon rank-sum and Fisher's exact tests, as appropriate, based on covariate distributions. Comparisons of DNA and RNA levels among strains were performed using the Wilcoxon rank-sum test and the Kruskal–Wallis test when two or three strains were being analysed, respectively. MIC comparisons were performed using ANOVA with Dunnett's test of multiple comparisons. Statistical significance was assigned as a two-sided *P* value <0.05.

Data availability

Assemblies of index isolates from patients with recurrent bacteraemia as well as long-read and short-read data for recurrent isolates have been deposited in the NCBI BioProject database (PRJNA603908). ONT sequencing data of non-CP-CRE isolates from a previous study[20] were deposited in the NCBI BioProject database (PRJNA388450).

Results

ESBL-E bacteraemia cohort

There were 116 patients with carbapenem-susceptible ESBL-E index bacteraemia cases. Clinical and demographic features are presented in Table S3. *E. coli* was the most common organism isolated (100/116; 86.2%), followed by *K. pneumoniae* (14/116; 12.1%) and *K. oxytoca* (2/116; 1.7%). Recurrent bacteraemia was identified in 16/116 (13.8%) patients and primarily occurred either in leukaemia or HSCT patients (14/16 cases, Table S3). Carbapenem-resistant isolates were present in 4/16 (25%) recurrent bacteraemia patients (Figure 1), with all four patients having *E. coli* serial isolates. Isolates from recurrent bacteraemia patients (*n* = 26) were available for analysis in 11/16 patients, including all strains from the four patients who had at least one recurrent isolate that developed a carbapenem-resistant phenotype.

Identification of recurrent bacteraemia E. coli isolates that developed carbapenem resistance

Short-read sequencing was performed on all 26 isolates (Table S4) from recurrent bacteraemia patients with clonality assessed initially via phylogenetic analysis (Figure S1). The date of infection, antimicrobial susceptibility and clonality status are depicted in Figure 1. We subsequently focused on recurrent bacteraemia isolates that developed carbapenem resistance to identify potential *de novo* mechanisms of carbapenem resistance. Three of the four carbapenem-resistant serial isolates (those from Patients 4, 10 and 11) had at least one non-CP-CRE recurrent strain. Our short-read WGS data indicated that for each of these three patients, their recurrent *E. coli* isolates clustered together within the phylogenetic tree, had the same Bayesian hierarchical population structure and belonged to the same ST (Figure S1). We generated long-read (ONT) plus short-read (Illumina) hybrid, consensus assemblies to create highly resolved genomes for the index strains of Patients 4, 10 and 11. We confirmed clonality by measuring pairwise SNP distances using these aforementioned genome assemblies and found less than 20 SNPs for all respective recurrent strains relative to their index strain, suggesting that these three patients had clonal strains that developed carbapenem resistance through a non-carbapenemase mechanism (Table 1). The other set of isolates in which carbapenem resistance developed (Patient 7, strains 7A–C) included both ST405 (7A–B) and ST10 (7C) isolates, with the latter isolate harbouring the class D carbapenemase $bla_{OXA-181}$, indicating that the patient had been infected with a new *E. coli* strain rather than the index strain developing carbapenem resistance.

E. coli isolates from Patient 4 (4A–D) and Patient 11 (11A–B) were ST131 whereas Patient 10 isolates (10A–C) were ST10. Each of the serial isolates had increased Illumina short-read and ONT long-read normalized coverage depth for β-lactamase genes indicating amplification (Table S5 and Table S6). Specifically, we identified increased normalized coverage depth of bla_{OXA-1} in all Patient 4 recurrent isolates, $bla_{CTX-M-55}$ (a derivative of $bla_{CTX-M-15}$ that differs by a single A80V amino acid substitution)[35] in Patient 10 recurrent isolates and bla_{OXA-1} and $bla_{CTX-M-15}$ in both the index and recurrent isolates of Patient 11 (Table 1). We used qPCR to confirm increased normalized coverage depth in our WGS analyses and qRT–PCR to show that the increased normalized coverage depth corresponded to increased transcript levels of the amplified β-lactamase genes for Patient 4 isolates (Figure 2) as well as Patient 10 and Patient 11 isolates (Figure S2). We further characterized outer membrane porin genes with sequencing data given
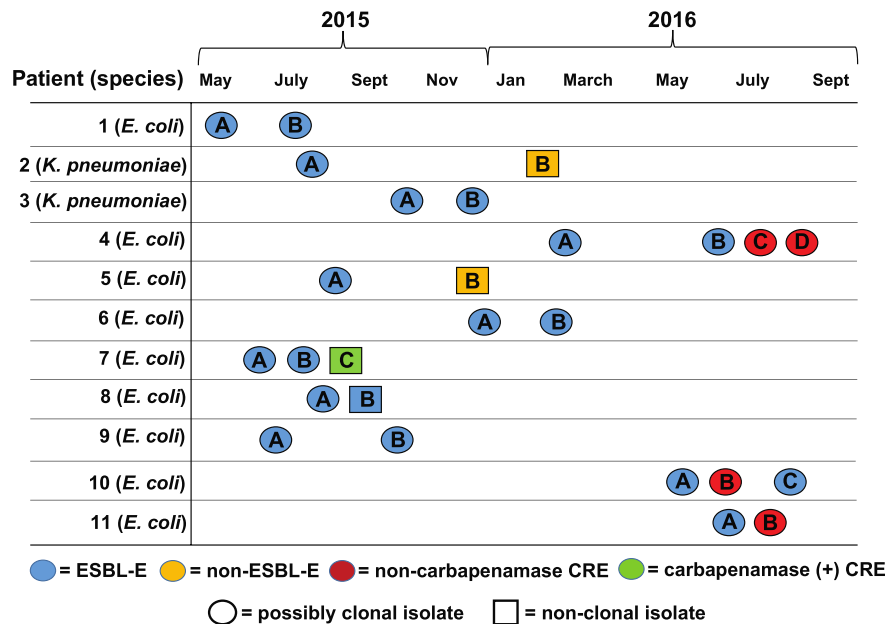
Figure 1. Timeline showing date of serial strain isolation from blood cultures. Patient numbers and species isolated are in the first column. The shape and colour of the isolate labels indicate potential clonality and AMR, respectively. Isolates were considered possibly clonal if they were the same ST and clustered on the phylogenetic tree presented in Figure S1. Patient subgroups (e.g. Patient 1; isolates A and B) refer to the order of isolation.

Table 1. Molecular and genomic characterization of clinical, recurrent bacteraemia Enterobacterales isolates

Patient	Isolate	ST	Species	Pairwise SNP distance	CAZ MIC[a]	FEP MIC[a]	TZP MIC[a]	ETP MIC[a]	MEM MIC[a]	ompC[b,c]	ompF[c,d]	β-lactamase amplification
4	4A	131	E. coli	Ref	16	>64	8	<0.5	<0.25	WT	WT	none
	4B	131	E. coli	2	16	8	>128	<0.5	<0.25	WT	WT	bla$_{OXA-1}$
	4C	131	E. coli	14	16	64	>128	>32	4	disruption[e]	disruption	bla$_{OXA-1}$
	4D	131	E. coli	15	>64	>64	>128	>32	4	disruption[e]	disruption	bla$_{OXA-1}$
10	10A	10	E. coli	Ref	16	2	8	<0.5	<0.25	WT	WT	none
	10B	10	E. coli	1	>64	>64	>128	>32	8	disruption	disruption	bla$_{CTX-M-55}$
	10C	10	E. coli	0	>64	>64	16	<0.5	<0.25	WT	WT	bla$_{CTX-M-55}$
11	11A	131	E. coli	Ref	>64	>64	64	<0.5	<0.5	intact[f]	disruption	bla$_{OXA-1}$, bla$_{CTX-M-15}$
	11B	131	E. coli	0	>64	>64	>128	4	1	disruption	disruption	bla$_{OXA-1}$, bla$_{CTX-M-15}$
NA	MB746	405	E. coli	NA	64	>64	>128	>32	4	disruption	disruption	bla$_{OXA-1}$, bla$_{CTX-M-15}$
NA	MB101	37	K. pneumoniae	NA	>64	>64	>128	>32	8	disruption[g]	disruption[g]	bla$_{OXA-1}$, bla$_{CTX-M-15}$

CAZ, ceftazidime; FEP, cefepime; TZP, piperacillin/tazobactam; ETP, ertapenem; MEM, meropenem; Ref, reference; NA, not available.
[a]All MICs reported in mg/L.
[b]UniProt reference entry names for ompC are A0A192C9D6_ECOLX, OMPC_ECOLI and U9Y7F2_ECOLX for ST131, ST10 and ST405 E. coli isolates, respectively; MB101 porin is ompK36 with UniProt reference entry name A0A0H3H0Y2_KLEPH.
[c]WT indicates WT coding DNA sequence, disruption indicates an INDEL event; all INDEL events are frameshift mutations that leave premature, truncated coding DNA sequences unless otherwise noted.
[d]UniProt reference entry names for ompF are A0A192CJU0_ECOLX, OMPF_ECOLI and S0Z171_ECOLX for ST131, ST10 and ST405 E. coli isolates, respectively; MB101 porin is ompK35 with UniProt reference entry name O87753_KLEPN.
[e]Insertion of MB1860TU_A with variable number of repeating units.
[f]INDEL, Y170_N174delinsKR, creates an in-frame OmpC protein.
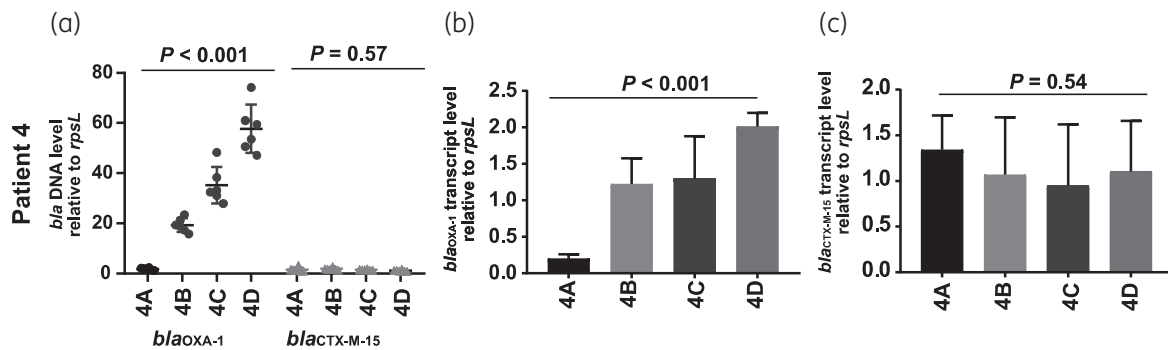[g]Insertion of 1× copy of MB101TPU in ompK36 and nonsense mutation (p.Y36X) in ompK35, respectively.

Figure 2. PCR analysis of β-lactamase gene levels and transcript levels for Patient 4 isolates (4A–D). (a) TaqMan qPCR of genomic DNA results collected in triplicate on two separate days ($n=6$) for either bla_{OXA-1} or $bla_{CTX-M-15}$ relative to the endogenous control gene *rpsL*. Data shown are individual data points with mean ± SD superimposed. (b) bla_{OXA-1} transcript level relative to endogenous control gene *rpsL*. RNA was collected from mid-exponential phase in triplicate on two separate days ($n=6$). Data shown are mean ± SD. (c) Similar analysis to (b) except that data are for $bla_{CTX-M-15}$. *P* values refer to measurements in the serial isolates relative to the initial isolate using the Kruskal–Wallis test.

that disruptions of these genes are correlated with carbapenem resistance.[2] We consistently identified that non-CP-CRE strains contained disruptions in the ORFs of porin proteins OmpC and OmpF (Table 1). We subsequently focused on the *E. coli* ST131 serial sets of isolates (i.e. Patient 4 and Patient 11 isolates) as both had non-CP-CRE mechanisms involving bla_{OXA-1} and $bla_{CTX-M-15}$ presence, potential amplification of these β-lactamase genes and porin disruption.

TnMB1860 present in both *E. coli* ST131 Patient 4 and Patient 11 index isolates

The consensus genome assemblies of index strains for Patient 4 (4A) and Patient 11 (11A) both contained an IS*26*-mediated translocatable unit (TU), herein designated as MB1860TU_A, which carried bla_{OXA-1}, adjacent and upstream of another TU, designated MB1860TU_B, which carried $bla_{CTX-M-15}$ (Figure 3a). MB1860TU_C is the combination of both TUs. The entire transposon structure, consisting of overlapping IS*26*-bounded transposons designated Tn*MB1860*, is shown in Figure 3a.

Tn*MB1860* is located on the chromosome of both index isolate 4A (GenBank accession #: CP049085) and index isolate 11A (GenBank accession #: CP049077). Variable-sized direct repeats called target site duplications (TSDs) flank ISs and are created during the transposition process.[36,37] The Tn*MB1860* transposon on the isolate 11A chromosome has 7 bp TSDs that indicate a transposition within an ORF that putatively is involved in molybdopterin cofactor biosynthesis (Figure S3). Tn*MB1860* in isolate 4A differs in chromosomal context relative to isolate 11A due to an IS*26*-mediated intramolecular transposition event that occurred in reverse orientation indicated by 8 bp TSDs at the breakpoint site of a colicin I receptor gene (Figure S4). An alignment of 4A and 11A isolates with two other *E. coli* ST131 chromosomes available from GenBank, TO217 (GenBank accession #: LS992192.1) and Ecol_AZ146 (GenBank accession #: CP018991.1) indicate similar chromosomal carriage of Tn*MB1860* with the noted inversion event that has occurred in isolate 4A (Figure S4). This alignment indicates that the strain 11A chromosome has comparable orientation with the aforementioned historical strain chromosomes, in contrast to the strain 4A chromosome, which has undergone an additional IS*26*-mediated transposition event.

Delineation of MB1860TU_A transposition in ST131 Patient 4 and Patient 11 serial isolates

Patient 11 isolates 11A and 11B had a relatively equal increase in normalized coverage depth for bla_{OXA-1} and $bla_{CTX-M-15}$ (Table S5). The consensus assemblies of both 11A and 11B isolates revealed that this increase in normalized coverage depth was due to two copies of bla_{OXA-1} and $bla_{CTX-M-15}$ being present on the chromosomal Tn*MB1860* as well as on IS*26*-mediated TUs present on a multireplicon, F-type plasmid, p11A_p2 (Figure S3, Figure S4; GenBank accession #: CP049079). The CRE phenotype of strain 11B relative to 11A appears to be driven by additional inactivation of the *ompC* gene via a frameshift, adenine insertion at position 131 of the coding sequence (CDS) of OmpC (c.131insA), given that the *ompF* gene is truncated by a deletion of 8 bp in the CDS of OmpF from nucleotide 305 to 312 (c.305_312del) in both strains (Table 1).

In contrast to the Patient 11 isolates, the transposition of the modular TUs that compose Tn*MB1860* in Patient 4 was present only in a chromosomal context (Figure 3). Within the Patient 4 serial isolates, there was a consistent increase in short-read normalized coverage depth (Figure 3a) of the entire MB1860TU_A structure harbouring bla_{OXA-1} up to approximately 23-fold in isolate 4D. We first analysed isolate 4B, which had developed resistance to piperacillin/tazobactam but remained carbapenem susceptible (Table 1). In isolate 4B, MB1860TU_A generated an ~10× tandem array *in situ* most likely through an IS*26*-mediated RecA-independent transposition mechanism or homologous recombination (Figure 3b).[38,39] The occurrence of the 10× TU amplification at the original Tn*MB1860* locus was confirmed by aligning the isolate 4B long reads to the reference chromosome of isolate 4A using SVAnts in conjunction with a short-read pileup analysis. All outer membrane porin genes remained intact in isolate 4B. Given that isolate 4B had developed resistance to piperacillin/ tazobactam relative to isolate 4A (Table 1), we sought to determine whether overexpression of bla_{OXA-1} could drive piperacillin/
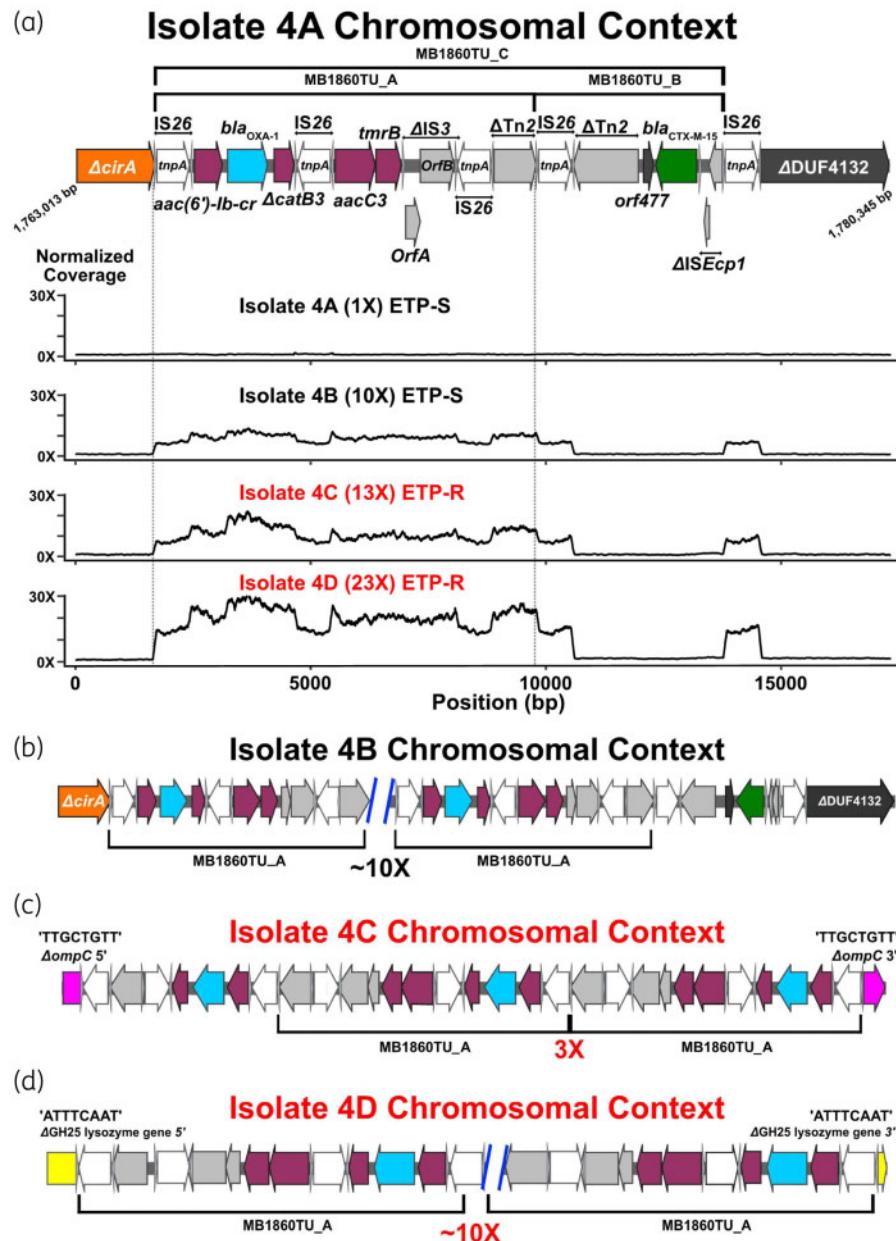
Figure 3. Characterization of IS*26*-flanked transposon, Tn*MB1860,* with transposition of modular TUs in Patient 4 serial isolates (i.e. isolates 4A–D). Terminal left and right inverted repeats (IR$_L$ and IR$_R$, respectively) of ISs are specified by grey triangles that bracket complete and incomplete *tnpA* genes, respectively. ORFs are coloured as follows: non-β-lactamase AMR genes (maroon), *bla*$_{OXA-1}$ (blue), *bla*$_{CTX-M-15}$ (green), IS*26 tnpA* (white) and other IS/Tn elements (grey). Font colour for each serial isolate labelled represents ertapenem susceptibility (black) or ertapenem resistance (red). (a) Schematic indicates chromosomal context (GenBank accession #: CP049085) of Tn*MB1860* locus flanked by directly oriented IS*26* transposases found in the 4A isolate. Immediately below the schematic are normalized, short-read coverage depth line graphs for the four Patient 4 serial isolates with MB1860TU_A bracketed by dotted lines. ETP-S, ertapenem susceptible; ETP-R, ertapenem resistant. (b–d) Characterization of MB1860TU_A transposition and ORF disruption events in each of the respective Patient 4 recurrent episode isolates. Black brackets beneath ORFs indicate MB168TU_A. (b) Isolate 4B chromosomal context shows an ~10× MB1860TU_A amplification event in the original 4A chromosomal locus. (c) Isolate 4C chromosomal context additionally contains transposition and disruption of the *ompC* porin gene (pink) upstream of the original isolate 4A *Tn*MB1860 locus with three copies of MB1860TU_A. (d) Isolate 4D has previous transposition events found in isolates 4B and 4C as well as another MB1860TU_A transposition, amplification and disruption of a putative glycoside hydrolase gene (i.e. GH25; yellow) downstream of the Tn*MB1860* locus. The TSDs created by the transposition of the TU are indicated above each respective junction site flanking the insertion and disruption of the *ompC* and *GH25* genes, respectively.
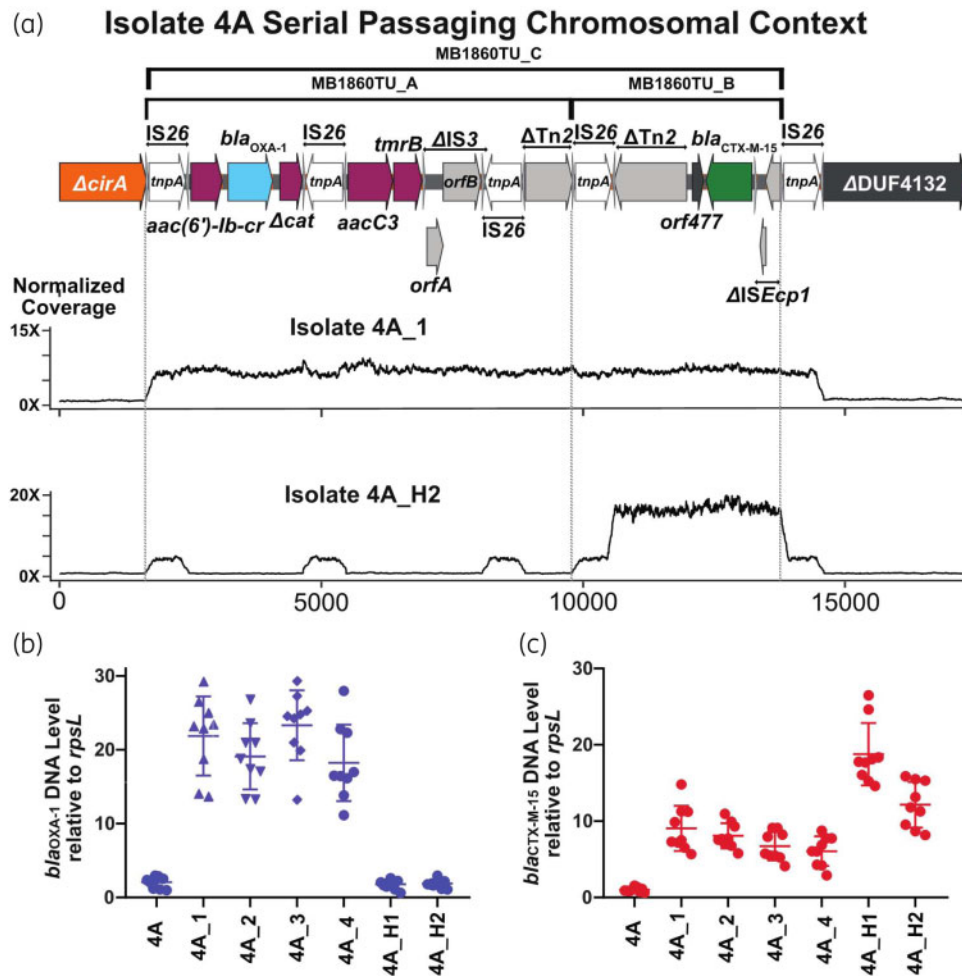
Figure 4. Identification and characterization of β-lactamase gene amplification following serial passaging of the index isolate 4A under ertapenem exposure. Isolate 4A was grown in the presence of ertapenem with isolates 4A_1 to 4A_4 collected during the first round of passaging and 4A_H1 and 4A_H2 collected during the second round. (a) Schematic of Tn*MB1860* locus from isolate 4A as detailed in Figure 3. Immediately below the schematic are normalized, short-read coverage depth line graphs for isolates 4A_1 and 4A_H2 aligned to index isolate 4A with the location of MB1860TU_A and MB1860TU_B bracketed by dotted lines. Note amplification of MB1860TU_C (i.e. MB1860TU_A and MB1860TU_C combined) in isolate 4A_1 whereas only MB1860TU_B is amplified in isolate 4A_H2. (b, c) TaqMan qPCR of genomic DNA collected in triplicate on two separate days ($n = 6$) for either bla_{OXA-1} (b) or bla_{CTX-M} (c) relative to the endogenous control gene *rpsL*. Data shown are individual data points with mean $\pm$ SD superimposed.

tazobactam resistance. Inducing bla_{OXA-1} expression through cloning under an arabinose-responsive promoter increased piperacillin/tazobactam MIC 6.8-fold relative to uninduced cells (Figure S5). Nevertheless, bla_{OXA-1} amplification in the absence of outer membrane porin disruption was not sufficient to drive carbapenem resistance in isolate 4B.

Next, we examined the non-CP-CRE serial isolates 4C and 4D. Interestingly, in both isolates 4C and 4D, a transposition and insertion of MB1860TU_A into *ompC* was present upstream of the original Tn*MB1860* chromosomal locus (Figure 3c). We found two individual long reads that were able to span the full length of the MB1860TU_A array (3× copies), which disrupts *ompC*, for isolate 4C as well as isolate 4D, and confirmed the exact MB1860TU insertion location within *ompC* (c.504_505ins; Table 1). We were also able to identify 8 bp TSDs (5′-TTGCTGTT-3′) at each end of the *ompC* insertion sites, which indicates MB1860TU_A replicative

transposition. The isolate 4D assembly and individual long reads indicated a second MB1860TU_A transposition and insertion ~67 kb downstream of Tn*MB1860* within a GH25 lysozyme gene (Figure 3d). This transposition event could be confirmed by 8 bp TSDs (5′-TTGCTGTT-3′) flanking the inverted repeats of IS*26* (Figure 3d). A progressive increase in both DNA and RNA levels for bla_{OXA-1} but not $bla_{CTX-M-15}$ in the Patient 4 serial isolates was confirmed using qPCR and qRT–PCR, respectively (Figure 2).

Serial passage of Patient 4 index strain

We passaged isolate 4A in increasing concentrations of ertapenem to determine whether antimicrobial exposure was driving the genetic changes observed in our serial clinical isolates. Resistance to ertapenem developed within three passages, corresponding to 3 days. Once ertapenem resistance developed, we collected

Table 2. Characterization of index isolate 4A serial passaging experiments

Sample	ETP MIC (mg/L)	*ompC*	*ompF*	*bla*OXA-1 copy #[a]	*bla*CTX-M-15 copy #[a]
4A	<0.5	WT	WT	1	1
4A_1	>32	c.208T>C; p. Q70X	c.17_18insIS*1A*	6	7
4A_2	>32	c.208T>C; p. Q70X	WT	8	9
4A_3	>32	c.208T>C; p. Q70X	insIS*1A*[b]	6	7
4A_4	>32	c.208T>C; p. Q70X	insIS*1A*[b]	6	7
4A_H1	>32	IS*1A*-mediated insertion 96 bp upstream of +1 *ompC* start site	WT	1	9
4A_H2	>32	IS*1A*-mediated insertion 96 bp upstream of +1 *ompC* start site	WT	1	17

ETP, ertapenem.
[a]See Materials and methods for normalized coverage depth calculations.
[b]Large IS*1A*-mediated deletion event (as described in Lee *et al.*)[51] at *ompF* insertion locus precludes the ability to note correct genomic context. This is due in part to multiple variable-sized deletions detected in the long-read data. This may reflect population heterogeneity or technical difficulties in resolving a single genomic deletion size.

strains for the next 4 days (4A_1 to 4A_4). ONT and Illumina sequencing on all four isolates indicated that, similar to isolate 4B, there was *in situ* amplification occurring at the original Tn*MB1680* chromosomal locus. However, the full-length TU MB1860TU_C (Figure 4a), which harbours both *bla*OXA-1 and *bla*CTX-M-15, was the amplifying structure for the passaged isolates in contrast to the clinical Patient 4 isolates where MB1860TU_A was the sole amplifying structure (Table 2). These results were confirmed with qPCR (Figure 4b).

We repeated the experiment and again found ertapenem resistance developed within three passages from the 4A isolate. ONT sequencing of the second round of passaged isolates (4A_H1 and 4A_H2) revealed amplification of MB1860TU_B, which harbours *bla*CTX-M-15 solely, which we verified using qPCR (Figure 4a and c). Similar to the clinical strains from Patient 4, the serially passaged ertapenem-resistant isolates contained inactivating mutations in *ompC*, although we did not observe any MB1860TU-mediated interruptions (Table 2). Differential INDELs inactivating the *ompF* gene were observed in a fraction of the serial isolates, suggesting *ompF* inactivation may not be necessary for the development of non-CP-CRE, as well as possible population heterogeneity (Table 2).

In order to determine the chromosomal stability of the MB1860TU tandem arrays in the absence of antibiotic selective pressure, both ertapenem-resistant isolates 4C and 4D were passaged for 10 days (∼60 generations) in the absence of ertapenem. Both ertapenem-resistant recurrent strains consistently maintained carbapenem resistance through 60 generations of growth (Figure S6). The 4C and 4D isolates had relative copy number decreases of *bla*OXA-1 from 33× to 18× (45% decrease) and 53× to 42× (21% decrease) respectively, but the amplifications remained substantially above the index isolate 4A baseline (Figure S6).

Detection of *β*-lactamase gene amplification and porin disruption by AMR elements in non-serial *Enterobacterales* strains

There were two non-CP-CRE strains, MB101 (*K. pneumoniae*) and MB746 (*E. coli*), identified in our previous study examining the role of short-read WGS in predicting β-lactam resistance in bacteraemia isolates (Table 1).[20] We performed ONT sequencing on these two isolates to determine whether mechanisms of gene amplification and porin disruption were similar to what we observed in the cohort of non-CP-CRE bacteraemia serial isolates. The chromosome of the *K. pneumoniae* (ST37) MB101 isolate contained amplified IS*26*-mediated TUs carrying *bla*OXA-1 nearly identical to MB1860TU_A (Figure 5a). Moreover, OmpK36, the homologue of OmpC in *E. coli*, was interrupted by a 5390 bp IS*Ecp1*-mediated transposition unit designated as MB101TPU (TPU; used here to delineate from IS*26*-mediated transposition mechanisms) harbouring *bla*CTX-M-15 (Figure 5b). The *E. coli* (ST405) MB746 isolate harboured a chromosomally amplified *bla*OXA-1 gene, as observed for Patient 4 serial isolates (Figure 5c), as well as a Tn*MB1860*-like element present on an F-type plasmid (Figure 5d). These results suggest the amplification/disruption mechanism may be prevalent in non-CP-CRE clinical isolates within the Houston region.

Discussion

While recent surveillance studies indicate that the prevalence of non-CP-CRE remains high,[4,5] mechanisms contributing to non-CP-CRE emergence within clinical settings are largely unknown. This public health issue is particularly troublesome given the recent finding of similar outcomes for patients with CPE and non-CP-CRE infections.[5] Over the past 7 years, there has been an estimated 50% increase in ESBL-E cases in the USA.[1] Given that non-CP-CRE is thought to evolve from ESBL-E precursor strains, there are concerns for a subsequent increase in non-CP-CRE infections. The CDC estimated in 2019 that 200 000 cases of ESBL-E infections and 13 000 cases of CRE infections occur in the USA annually.[1] Assuming 50% of CRE are non-CP-CRE,[4,5] the potential fraction of ESBL-E cases that develop into non-CP-CRE is approximately 3%, which is comparable with what we observed in our cohort. One of the commonly observed ESBL-E organisms detected is the pandemic, extraintestinal pathogenic *E. coli* ST131 group.[40] Therefore, it was concerning that we identified two distinct ST131, non-CP-
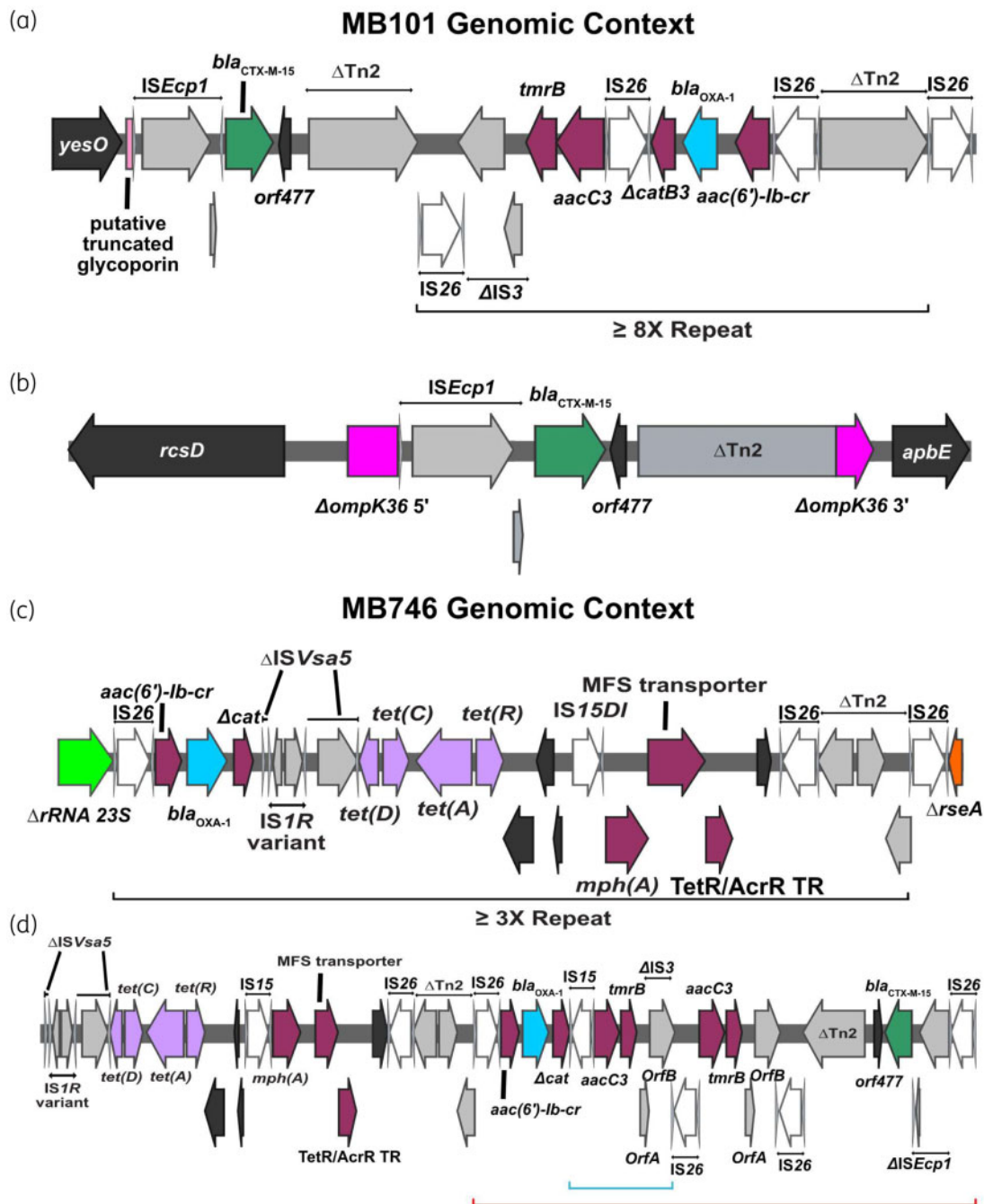
Figure 5. Genomic context of MB101 (*K. pneumoniae*) and MB746 (*E. coli*) isolates respectively. Terminal left and right inverted repeats (IR$_L$ and IR$_R$, respectively) of ISs are specified by grey triangles that bracket complete and incomplete *tnpA* genes, respectively. ORFs are coloured as follows: AMR genes (maroon), *bla*$_{OXA-1}$ (blue), *bla*$_{CTX-M-15}$ (green), IS26 *tnpA* (white) and other IS/Tn elements (grey). Delta (Δ) next to an annotated gene or genetic region indicates a truncation or disruption. (a, b) Chromosomal locations of MB101TU (a) and MB101TPU (b) indicating amplification and transposition of each element, respectively. The black bracket indicates an ∼8× MB101TU repeat. Truncated *ompK36* gene (b) is labelled in pink. (c, d) Genomic context of MB746TU and respective modules carrying AMR genes. Black brackets beneath (c) schematic indicate repeating MB746TU. (d) shows FIB plasmid carriage of AMR gene-containing modules. The red bracket indicates an IS26-bounded transposon structure that shares 100% coverage; 99% BLAST similarity with Tn*MB1860*. The blue bracket indicates a small, 2× repeat structure.

CRE isolates containing similar TUs harbouring β-lactamase genes and nearly identical TUs were present in previously sequenced ST131 isolates present in GenBank.

Through a combination of comparative genomic methods using clinical isolates and laboratory passaging of an index clinical *E. coli* ST131 isolate, we demonstrate that IS26-mediated modular

amplifications of β-lactamase genes in conjunction with porin inactivation can drive non-CP-CRE emergence. We show that the TUs mediating β-lactamase gene amplification can translocate and disrupt porin genes, thereby simultaneously augmenting β-lactamase production and reducing antimicrobial entry into the periplasmic space. Moreover, our own results from serial passaging of clinical non-CP-CRE isolates without ertapenem exposure suggest that these amplified structures harbouring AMR genes associated with increased ertapenem and meropenem MICs may be fairly stable in the absence of antibiotic selective pressure. These results stand in contrast to the unstable nature of AMR gene amplifications observed following laboratory passaging of clinical isolates,[34,41] but are in line with our identification of several non-CP-CRE clinical isolates with β-lactamase gene amplification causing serious infections.

It has long been recognized that increasing gene copy number can expand the range of AMR for a given β-lactamase,[42–44] but the genetic complexity of such amplifications has hindered direct observations of mechanisms driving resistance, particularly in clinical isolates.[45] While there have been a number of studies that have implicated IS-mediated porin disruptions,[46–50] this is, to our knowledge, the first documented IS*26*-mediated TU disruption of an outer membrane porin with a tandem array of β-lactamase genes. Given the length of the TUs and their ability to generate tandem arrays, it is unlikely that targeted PCR-based strategies or commonly used short-read approaches alone would have been able to identify the correct genomic context underlying this particular non-CP-CRE mechanism. Future studies to determine signalling pathways that regulate and activate TU-mediated transposition, particularly into DNA motifs within outer membrane porins, are warranted. We predict that more widespread application of long-read sequencing technologies will facilitate appreciation of TU- and TPU-mediated transpositions, porin disruptions and gene amplifications on a diverse array of AMR pathogens in the clinical setting.

Acknowledgements

Funding

Transparency declarations
No competing interests to declare.

Supplementary data
Supplementary methods, Supplementary references, Tables S1–S6 and Figures S1–S6 are available as Supplementary data at *JAC* Online.

References
1 CDC. Antibiotic Resistance Threats in the United States 2019. 2019. https://www.cdc.gov/drugresistance/pdf/threats-report/2019-ar-threats-report-508.pdf

2 Logan LK, Weinstein RA. The epidemiology of carbapenem-resistant Enterobacteriaceae: the impact and evolution of a global menace. *J Infect Dis* 2017; **215**: S28–36.

3 Nordmann P, Naas T, Poirel L. Global spread of carbapenemase-producing Enterobacteriaceae. *Emerg Infect Dis* 2011; **17**: 1791–8.

4 Guh AY, Bulens SN, Mu Y *et al.* Epidemiology of carbapenem-resistant Enterobacteriaceae in 7 US communities, 2012-2013. *JAMA* 2015; **314**: 1479–87.

5 van Duin D, Arias CA, Komarow L *et al.* Molecular and clinical epidemiology of carbapenem-resistant Enterobacterales in the USA (CRACKLE-2): a prospective cohort study. *Lancet Infect Dis* 2020; **20**: 731–41.

6 Su CF, Chuang C, Lin YT *et al.* Treatment outcome of non-carbapenemase-producing carbapenem-resistant *Klebsiella pneumoniae* infections: a multicenter study in Taiwan. *Eur J Clin Microbiol Infect Dis* 2018; **37**: 651–9.

7 Hayakawa K, Nakano R, Hase R *et al.* Comparison between IMP carbapenemase-producing Enterobacteriaceae and non-carbapenemase-producing Enterobacteriaceae: a multicentre prospective study of the clinical and molecular epidemiology of carbapenem-resistant Enterobacteriaceae. *J Antimicrob Chemother* 2020; **75**: 697–708.

8 Hamzaoui Z, Ocampo-Sosa A, Fernandez Martinez M *et al.* Role of association of OmpK35 and OmpK36 alteration and *bla*~ESBL~ and/or *bla*~AmpC~ genes in conferring carbapenem resistance among non-carbapenemase-producing *Klebsiella pneumoniae. Int J Antimicrob Agents* 2018; **52**: 898–905.

9 Oteo J, Delgado-Iribarren A, Vega D *et al.* Emergence of imipenem resistance in clinical *Escherichia coli* during therapy. *Int J Antimicrob Agents* 2008; **32**: 534–7.

10 Poirel L, Heritier C, Spicq C *et al.* In vivo acquisition of high-level resistance to imipenem in *Escherichia coli. J Clin Microbiol* 2004; **42**: 3831–3.

11 Goessens WH, van der Bij AK, van Boxtel R *et al.* Antibiotic trapping by plasmid-encoded CMY-2 β-lactamase combined with reduced outer membrane permeability as a mechanism of carbapenem resistance in *Escherichia coli. Antimicrob Agents Chemother* 2013; **57**: 3941–9.

12 Tangden T, Adler M, Cars O *et al.* Frequent emergence of porin-deficient subpopulations with reduced carbapenem susceptibility in ESBL-producing *Escherichia coli* during exposure to ertapenem in an *in vitro* pharmacokinetic model. *J Antimicrob Chemother* 2013; **68**: 1319–26.

13 van Boxtel R, Wattel AA, Arenas J *et al.* Acquisition of carbapenem resistance by plasmid-encoded-AmpC-expressing *Escherichia coli. Antimicrob Agents Chemother* 2017; **61**: e01413-16.

14 Adler M, Anjum M, Andersson DI *et al.* Influence of acquired β-lactamases on the evolution of spontaneous carbapenem resistance in *Escherichia coli. J Antimicrob Chemother* 2013; **68**: 51–9.

15 Kao CY, Chen JW, Liu TL *et al.* Comparative genomics of *Escherichia coli* sequence type 219 clones from the same patient: evolution of the IncI1 *bla*~CMY~-carrying plasmid in vivo. *Front Microbiol* 2018; **9**: 1518.

16 Dupont H, Choinier P, Roche D *et al.* Structural alteration of OmpR as a source of ertapenem resistance in a CTX-M-15-producing *Escherichia coli* O25b:H4 sequence type 131 clinical isolate. *Antimicrob Agents Chemother* 2017; **61**: e00014-17.

17 Chia JH, Siu LK, Su LH *et al.* Emergence of carbapenem-resistant *Escherichia coli* in Taiwan: resistance due to combined CMY-2 production and porin deficiency. *J Chemother* 2009; **21**: 621–6.

18 Harris PA, Taylor R, Thielke R *et al.* Research electronic data capture (REDCap)—a metadata-driven methodology and workflow process for providing translational research informatics support. *J Biomed Inform* 2009; **42**: 377–81.

19 CLSI. *Performance Standards for Antimicrobial Susceptibility Testing—Twenty-EighthEdition : M100.* 2018.

20 Shelburne SA, Kim J, Munita JM *et al.* Whole-genome sequencing accurately identifies resistance to extended-spectrum β-lactams for major Gram-negative bacterial pathogens. *Clin Infect Dis* 2017; **65**: 738–45.

21 Li H. Aligning sequence reads, clone sequences and assembly contigs with BWA-MEM. *arXiv* 2013; https://arxiv.org/pdf/1303.3997.pdf.

22 Li H. Minimap2: pairwise alignment for nucleotide sequences. *Bioinformatics* 2018; **34**: 3094–100.

23 Li H, Handsaker B, Wysoker A *et al.* The Sequence Alignment/Map format and SAMtools. *Bioinformatics* 2009; **25**: 2078–9.

24 Kolmogorov M, Yuan J, Lin Y *et al.* Assembly of long, error-prone reads using repeat graphs. *Nat Biotechnol* 2019; **37**: 540–6.

25 Page AJ, Cummins CA, Hunt M *et al.* Roary: rapid large-scale prokaryote pan genome analysis. *Bioinformatics* 2015; **31**: 3691–3.

26 Löytynoja A. *Phylogeny-Aware Alignment with PRANK.* Humana Press, 2014.

27 Stamatakis A. RAxML version 8: a tool for phylogenetic analysis and post-analysis of large phylogenies. *Bioinformatics* 2014; **30**: 1312–3.

28 Jolley KA, Maiden MC. BIGSdb: scalable analysis of bacterial genome variation at the population level. *BMC Bioinformatics* 2010; **11**: 595.

29 Seemann T. Prokka: rapid prokaryotic genome annotation. *Bioinformatics* 2014; **30**: 2068–9.

30 Jia B, Raphenya AR, Alcock B *et al.* CARD 2017: expansion and model-centric curation of the comprehensive antibiotic resistance database. *Nucleic Acids Res* 2017; **45**: D566–73.

31 Carattoli A, Zankari E, Garcia-Fernandez A *et al.* In silico detection and typing of plasmids using PlasmidFinder and plasmid multilocus sequence typing. *Antimicrob Agents Chemother* 2014; **58**: 3895–903.

32 Siguier P, Perochon J, Lestrade L *et al.* ISfinder: the reference centre for bacterial insertion sequences. *Nucleic Acids Res* 2006; **34**: D32–6.

33 Hanson B, Johnson J, Leopold S *et al.* SVants—a long-read based method for structural variation detection in bacterial genomes. *bioRxiv* 2019: 822312.

34 Adler M, Anjum M, Berg OG *et al.* High fitness costs and instability of gene duplications reduce rates of evolution of new genes by duplication-divergence mechanisms. *Mol Biol Evol* 2014; **31**: 1526–35.

35 He D, Chiou J, Zeng Z *et al.* Residues distal to the active site contribute to enhanced catalytic activity of variant and hybrid β-lactamases derived from CTX-M-14 and CTX-M-15. *Antimicrob Agents Chemother* 2015; **59**: 5976–83.

36 Partridge SR. Analysis of antibiotic resistance regions in Gram-negative bacteria. *FEMS Microbiol Rev* 2011; **35**: 820–55.

37 He S, Hickman AB, Varani AM *et al.* Insertion sequence IS*26* reorganizes plasmids in clinically isolated multidrug-resistant bacteria by replicative transposition. *mBio* 2015; **6**: e00762-15.

38 Harmer CJ, Hall RM. IS*26*-mediated formation of transposons carrying antibiotic resistance genes. *mSphere* 2016; **1**: e00038-16.

39 Harmer CJ, Moran RA, Hall RM. Movement of IS*26*-associated antibiotic resistance genes occurs via a translocatable unit that includes a single IS*26* and preferentially inserts adjacent to another IS*26*. *mBio* 2014; **5**: e01801-14.

40 Stoesser N, Sheppard AE, Pankhurst L *et al.* Evolutionary history of the global emergence of the *Escherichia coli* epidemic clone ST131. *mBio* 2016; **7**: e02162-15.

41 Nicoloff H, Hjort K, Levin BR *et al.* The high prevalence of antibiotic hetero-resistance in pathogenic bacteria is mainly caused by gene amplification. *Nat Microbiol* 2019; **4**: 504–14.

42 Normark S, Edlund T, Grundstrom T *et al. Escherichia coli* K-12 mutants hyperproducing chromosomal β-lactamase by gene repetitions. *J Bacteriol* 1977; **132**: 912–22.

43 Sandegren L, Andersson DI. Bacterial gene amplification: implications for the evolution of antibiotic resistance. *Nat Rev Microbiol* 2009; **7**: 578–88.

44 Bradford PA, Urban C, Mariano N *et al.* Imipenem resistance in *Klebsiella pneumoniae* is associated with the combination of ACT-1, a plasmid-mediated AmpC β-lactamase, and the foss of an outer membrane protein. *Antimicrob Agents Chemother* 1997; **41**: 563–9.

45 Livermore DM, Day M, Cleary P *et al.* OXA-1 β-lactamase and non-susceptibility to penicillin/β-lactamase inhibitor combinations among ESBL-producing *Escherichia coli. J Antimicrob Chemother* 2019; **74**: 326–33.

46 Hernández-Allés S, Benedí VJ, Martínez-Martínez L *et al.* Development of resistance during antimicrobial therapy caused by insertion sequence interruption of porin genes. *Antimicrob Agents Chemother* 1999; **43**: 937–9.

47 Doumith M, Ellington MJ, Livermore DM *et al.* Molecular mechanisms disrupting porin expression in ertapenem-resistant *Klebsiella* and *Enterobacter* spp. clinical isolates from the UK. *J Antimicrob Chemother* 2009; **63**: 659–67.

48 Vandecraen J, Chandler M, Aertsen A *et al.* The impact of insertion sequences on bacterial genome plasticity and adaptability. *Crit Rev Microbiol* 2017; **43**: 709–30.

49 Mena A, Plasencia V, Garcia L *et al.* Characterization of a large outbreak by CTX-M-1-producing *Klebsiella pneumoniae* and mechanisms leading to in vivo carbapenem resistance development. *J Clin Microbiol* 2006; **44**: 2831–7.

50 Zowawi HM, Forde BM, Alfaresi M *et al.* Stepwise evolution of pandrug-resistance in *Klebsiella pneumoniae. Sci Rep* 2015; **5**: 15082.

51 Lee H, Doak TG, Popodi E *et al.* Insertion sequence-caused large-scale rearrangements in the genome of *Escherichia coli. Nucleic Acids Res* 2016; **44**: 7109–19.